



**REVIEW**

 Cite this: *RSC Adv.*, 2023, 13, 3947

# A critical review of silicon nanowire electrodes and their energy storage capacities in Li-ion cells

 C. Yang  and K. S. Ravi Chandran \*

The electrochemical performances of silicon nanowire (SiNW) electrodes with various nanowire forms, intended as potential negative electrodes for Li-ion batteries, are critically reviewed. The lithium storage capacities, cycling performance, and how the volume expansion is possibly accommodated in these structures are discussed. The SiNW morphology can have a greater impact on the energy storage capacity and cycling performance if the parameters affecting the performance are clearly identified, which is the objective of this review. It is shown that the specific capacity measure is not adequate to truly assess the potential of an electrode and the necessity of the areal capacity measure is highlighted. It is shown that both measures are essential for the assessment of the true potential of a SiNW electrode relative to competing electrodes. Si mass loading in SiNWs has been found to be important for areal and specific capacities. An increase of mass loading of SiNWs is shown to increase the areal capacity significantly, but the specific capacity is found to decrease in thicker Si electrodes. Further, modifications of SiNW electrodes, with coating and doping, have shown significant increases in the performance of these electrodes in Li-ion batteries. The SiNW electrodes, to date, are far below the areal capacity of 3 mA h cm<sup>-2</sup>, which may be the minimum threshold capacity for a promising SiNW electrode with respect to Li-ion batteries.

 Received 18th November 2022  
 Accepted 20th January 2023

DOI: 10.1039/d2ra07326a

[rsc.li/rsc-advances](https://rsc.li/rsc-advances)

## 1. Introduction

Rapid growth in electric vehicles and portable electronic devices has increased the need for high energy density Li-ion batteries

with good cycling stability over thousands of charge–discharge cycles. The state-of-the-art Li-ion batteries (LIBs), with graphite as the anode and LiCoO<sub>2</sub> as the cathode, are limited to energy densities of the order of ~150 W h kg<sup>-1</sup> (~375 W h L<sup>-1</sup>).<sup>1</sup> These cannot meet the rising demands of long-range electric vehicles as there is no scope to improve the areal capacity or energy density further with C–LiCoO<sub>2</sub> chemistry. Therefore, it is

*Department of Materials Science and Engineering, The University of Utah, Salt Lake City, UT-84112, USA. E-mail: ravi.chandran@utah.edu*



*Chenguang Yang received his B.S. in Materials Science and Engineering from Tianjin University in 2016, and he received his M.S. in Materials Science and Engineering from University of California, Davis in 2018. He is currently pursuing his PhD in Metallurgical Engineering at the University of Utah. His current research topic is on Si anode material for lithium-ion batteries.*



*Dr Ravi Chandran is a Professor in the Department of Materials Science and Engineering at the University of Utah. He received his PhD degree from Indian Institute of Science. His research includes Li-ion batteries, mechanical behavior, alloy development and computational material science. Dr Chandran received several awards including the Champion Mathewson Award TMS and three*

*times the outstanding teaching awards of the MSE department. He is author of over 160 publications and over 120 presentations, both invited and contributed. He has graduated over 30 graduate students. He is a Fellow of ASM International, and member of ECS, MRS, TMS.*



necessary to focus on new electrode materials to develop negative electrodes with higher capacity and energy density for LIBs. In this context, Si has attracted a lot of attention as a negative electrode material, because of its high theoretical capacity ( $4200 \text{ mA h g}^{-1}$ ), which is about 10 times higher than graphite ( $372 \text{ mA h g}^{-1}$ ).<sup>2</sup> However, Si suffers from a large volumetric expansion ( $\sim 300\%$ ) during lithiation, which leads to electrode cracking and fragmentation.<sup>3</sup> This has been a major technical barrier in the development of practical Li-ion batteries based on Si electrodes. Besides, the relatively slow diffusion of Li in Si (Si is a non-intercalating material for Li) is also a challenge from a point of view of reaching full capacity in Si at a large C-rate.<sup>4</sup> To solve these problems, a significant amount of work has been done on creating nano-scale Si structures that can provide high Li-storage capacity and have the ability to accommodate the volume expansion. Si electrodes with various microscale morphologies of Si have been explored, including Si nanoparticles,<sup>5–7</sup> Si nanowires,<sup>8–10</sup> Si thin films<sup>11,12</sup> and columnar Si structures.<sup>13,14</sup>

Among various morphologies of Si electrodes, one-dimensional (1D) silicon nanowires (SiNWs) are of high interest because they can allow the lateral expansion of Si upon lithiation in free space between the wires.<sup>8</sup> This can potentially minimize cracking due to the volume change during lithiation. In Si nanowires, electrical transport along the wire axis is facilitated while Li-ion transport during charging and discharging is possible in the transverse direction, with a short diffusion distance.<sup>15</sup> These characteristics highly favor SiNW electrodes for achieving superior capacities and energy densities,<sup>16–18</sup> but clearly they need to be further improved for a practical Li-ion battery.

The synthesis of SiNWs was first reported by Wagner and Ellis in 1964, where the growth of Si nanowires was catalyzed by gold particles.<sup>19</sup> Since then, various growth techniques for SiNWs have been developed. The most common approach is chemical vapor deposition (CVD), where silane is used as the source of Si. Au particles, deposited on a substrate served as the catalyst promoting nanowire growth. The CVD processes provide flexibility to achieve an optimal nanowire structure where the length, diameter and orientation of SiNWs can be controlled by doping and by varying process parameters.<sup>20</sup>

Another common method to synthesize SiNWs is metal-assisted chemical etching (MACE), where noble metal (Au, Ag, Pt, *etc.*) particles are deposited onto Si substrate first. For example, Ag particles can be deposited by reacting Si surface with a solution mixture of HF and  $\text{AgNO}_3$ .<sup>21</sup> In the second step, an etching solution is used to create Si nanowires on the substrate. During etching, the noble metal directs the etching front into the Si substrate, resulting in the formation of nanowires. The parameters of the noble metal particles control the etching rate and the size of the SiNWs. This catalyst-controlled directional etching in the MACE process can create vertically-aligned SiNWs with high aspect ratio at a low fabrication cost.<sup>22</sup> Additionally, process modifications such as doping and coating have helped to improve the electrochemical performances of SiNW electrode.<sup>23–25</sup> Therefore, the variety of synthesis methods and the modification techniques available

for SiNW growth provide a great opportunity to develop practical SiNW electrodes for LIBs.

There are several publications reporting the performances of SiNW electrodes,<sup>26–28</sup> and notably, two review articles.<sup>29,30</sup> However, the reviews simply summarized the forms of SiNW electrodes and their electrochemical performances, without a critical assessment of the data. Specifically, a meaningful comparison of the relative performances of different SiNW electrodes should be based on both specific capacity ( $\text{mA h g}^{-1}$ ) and areal capacity ( $\text{mA h cm}^{-2}$ ) metrics, which have not been performed before in the literature. In fact, in some SiNW electrodes, the achievement of a high specific capacity (which is less significant than the areal capacity in the context of practical LIBs) has been at the cost of the areal capacity of the electrode. Therefore, a critical assessment of the relative merits of the SiNW electrodes with various nanowire structures, on both specific and areal capacity basis, is needed to get a comprehensive picture of the relative performances and their limits.

In this review, several unique SiNW morphologies and their performances in LIBs have been critically evaluated. The specific and areal capacity data from the selected works are compared to determine the relative merits in terms of long-term performance. This review is intended to provide important insights for further structural optimization of SiNW electrodes for Li-ion batteries.

## 2. Compilation of structures and performances of various SiNW electrodes

In reviewing the SiNW structures reported in literature, one finds a fascinating array of SiNW structures prepared by various synthesis or deposition techniques. In this section, the morphological features and the synthesis methods are discussed first as a background preparation. This is needed to understand the variations in electrochemical performances reported in the next section.

The microstructures of selected SiNW electrodes are shown in Fig. 1 and 2. Fig. 1(a) presents the morphology of pure Si nanowires synthesized by hot-filament chemical vapor deposition (HF-CVD) technique.<sup>31</sup> The SiNWs were grown on stainless steel substrate ( $50 \mu\text{m}$  thickness) with  $\text{SiH}_4$  as the precursor at a temperature of  $540 \text{ }^\circ\text{C}$ . The substrate with the SiNWs was then cut into small pieces ( $\sim 0.25 \text{ cm}^2$ ) and used as negative electrodes in Li-ion cells.

Fig. 1(b) illustrates the structure of Cu-coated SiNWs.<sup>32</sup> This nanowire electrode was synthesized by CVD on a stainless-steel substrate maintained at  $540 \text{ }^\circ\text{C}$ . After CVD, a copper coating (thickness  $\sim 10 \text{ nm}$ ) was deposited by magnetron sputtering. The SiNWs with Cu coating had an average diameter of  $\sim 100 \text{ nm}$ . X-ray diffraction analysis showed that these SiNWs were highly crystalline.

Fig. 1(c) is a scanning electron microscope (SEM) image of porous SiNWs prepared by the etching of boron-doped Si wafer with a solution mixture containing  $0.02 \text{ M AgNO}_3$  and  $5 \text{ M HF}$ .<sup>33</sup> The average pore diameter and wall thickness in the SiNWs

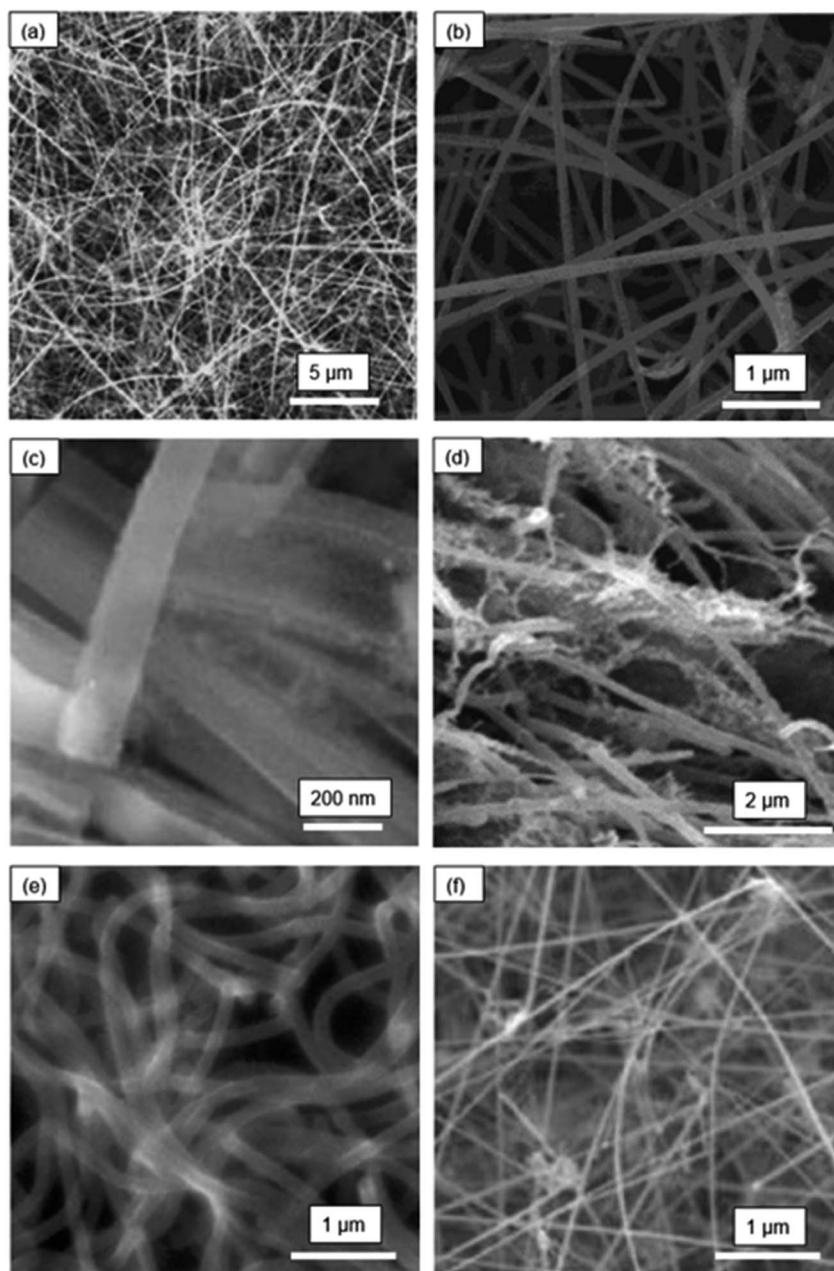


**Fig. 1** Morphologies of SiNW electrodes: (a) pure SiNWs (Leveau *et al.*;<sup>34</sup> reproduced with permission from Elsevier) (b) Cu-coated SiNWs (Chen *et al.*;<sup>32</sup> reproduced with permission from Elsevier) (c) boron-doped porous SiNWs (Ge *et al.*;<sup>33</sup> reproduced with permission from American Chemical Society) (d) kinked-SiNWs (Georgiana *et al.*;<sup>34</sup> reproduced with permission from Springer Nature) (e) crystalline-amorphous core-shell SiNWs (Cui *et al.*;<sup>35</sup> reproduced with permission from American Chemical Society) (f) carbon nanotube-enhanced SiNWs (Li *et al.*;<sup>36</sup> reproduced with permission from John Wiley and Sons).

were  $\sim 8$  nm and  $\sim 6$  nm, respectively. These pores here are too small to be seen in the SEM image in Fig. 1(c), but they are seen in the high-resolution TEM images provided in this work. The SiNW electrodes for Li-ion cell cycling were prepared by slurry casting of the SiNWs scrapped from the substrate. The scrapped SiNWs were first mixed with super-P conductive carbon black and alginate binder in water and the slurry was then cast on copper foils to make the electrodes. The advantage of the slurry casting approach is that it is compatible with the production process of commercial LIBs, where the mass loading of Si can be

precisely controlled. However, the mixing and casting can also mechanically damage SiNWs compromising their structural integrity.

Fig. 1(d) shows the interwoven and kinked silicon nanowire (k-SiNW) structure that was synthesized by MACE followed by chemical detachment from the substrate.<sup>34</sup> In the first step of synthesis, a gold mask with patterned holes was created on Si substrate by photolithography. The substrate with the mask was then exposed to an etchant comprising HF and H<sub>2</sub>O<sub>2</sub>. The SiNW structure was obtained by a repetitive etch and rinse sequence.

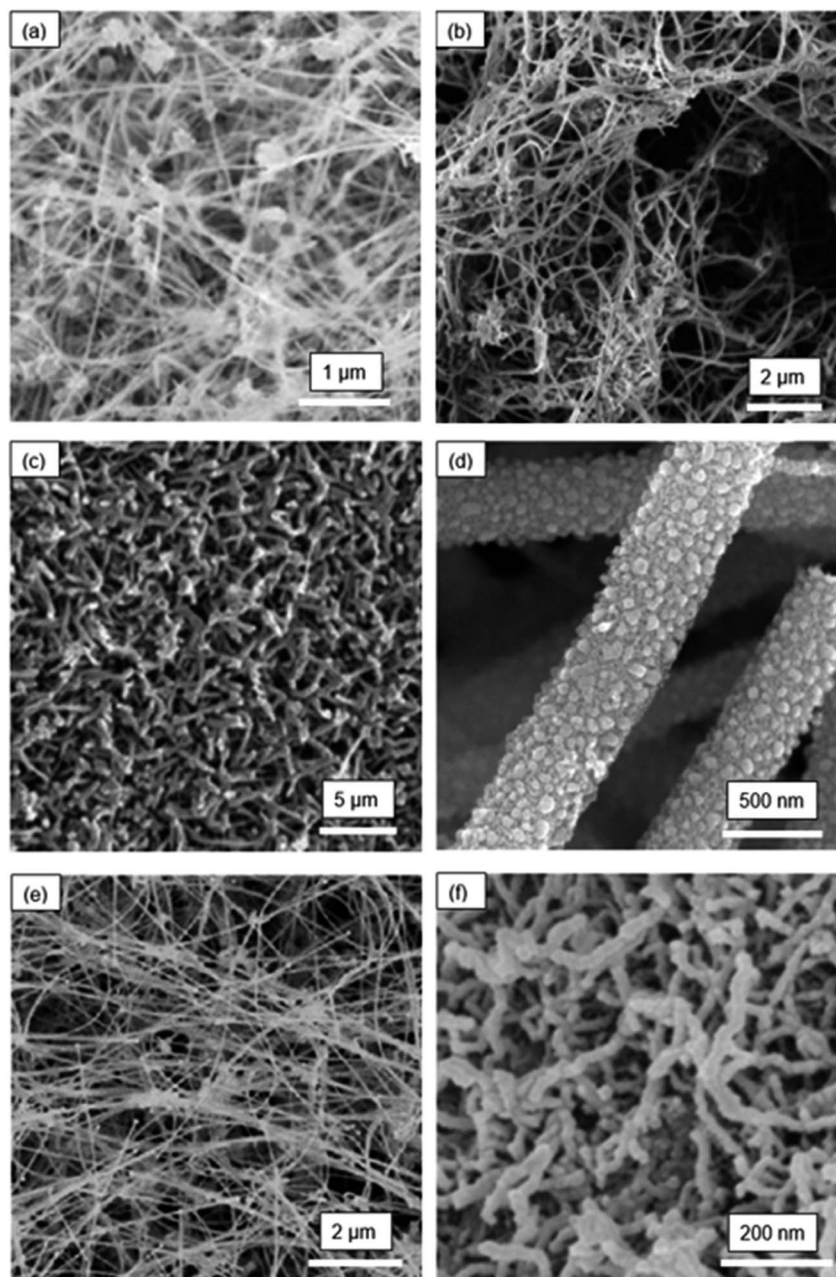


Fig. 2 Morphologies of SiNW electrodes: (a) SiNW fabric (Chockla *et al.*;<sup>37</sup> reproduced with permission from American Chemical Society) (b) carbon-coated SiNWs mixed with MWNTs (Chan *et al.*;<sup>38</sup> reproduced with permission from American Chemical Society) (c) coral-like SiNWs (Wang *et al.*;<sup>39</sup> reproduced with permission from American Chemical Society) (d) porous SiNWs (Yoo *et al.*;<sup>40</sup> reproduced with permission from IOP Publishing) (e) template-grown SiNWs (Cho *et al.*;<sup>41</sup> reproduced with permission from American Chemical Society) (f) electrodeposited SiNWs (Weng *et al.*;<sup>42</sup> reproduced with permission from American Chemical Society).

The substrate was rinsed in methanol every 5 min of etching to promote the development of a high-aspect-ratio SiNW structure. The resulting SiNW architecture was attached to the substrate. In addition, multi-walled carbon nanotubes (MWCNTs) were integrated with the SiNW structure in the electrodes to serve as a conductive media.

Fig. 1(e) shows the structure of crystalline-core and amorphous-shell SiNWs that were grown directly on a stainless-steel substrate, without any catalyst, by a simple one-step CVD process.<sup>35</sup> The silicon nanowires were grown by flowing SiH<sub>4</sub>/Ar

gas (2% SiH<sub>4</sub>) at a temperature between 460 and 510 °C, in the CVD reactor. This study determined that a relatively high pressure and high temperature in the reactor, as well as a high flow rate of SiH<sub>4</sub>, led to the formation of c-a core-shell SiNW structure. In this structure, the crystalline Si core was encapsulated by an exterior shell made of amorphous Si. Crystalline Si core functions as a stable mechanical support and an efficient electrical conducting pathway while the amorphous Si shell is largely involved in lithiation/delithiation.

Fig. 1(f) shows the structure of SiNWs grown by CVD using a structural base made of a carbon nanotube (CNT) and Au nanoparticle hybrid network.<sup>36</sup> Here, the CNT-Au network was used to nucleate and grow the SiNWs. After the growth, the CNTs and SiNWs formed a three-dimensional and electrically conductive network, providing a robust electrical contact with the current collector.

Fig. 2 shows the SEM images of the six other morphologies of SiNW-based electrodes.<sup>37</sup> Fig. 2(a) presents an interesting fabric-like network architecture of SiNWs that was prepared as an electrode for LIBs. Here, the SiNW structure was made by supercritical-fluid-liquid-solid (SFLS) growth technique with gold nanocrystals working as catalysts for SiNW growth. The resulting SiNW fabric is composed of highly entangled SiNWs in an electrode of  $\sim 50 \mu\text{m}$  in thickness. This is a highly porous structure with a good electrical connectivity to the base.

Fig. 2(b) is carbon-coated SiNWs prepared by a version of the SFLS process.<sup>38</sup> The carbon coating on this SiNW structure was achieved by carbonization of a sucrose precursor. The carbon coating enabled good electrical contact between SiNWs and the current collector. In addition, multiwalled carbon nanotubes were used as an additive to increase the conductivity of the electrode.

Fig. 2(c) shows the SiNW electrode with a coral-like SiNW network.<sup>39</sup> This SiNW structure was prepared by plasma-enhanced CVD (PECVD) process, using a stainless-steel substrate. In the PECVD,  $\text{PH}_3$  gas was also introduced in the

deposition chamber to dope the growing SiNWs with P. The objective was to improve the electrical conductivity of the SiNWs by doping. After PECVD, the electrodes with SiNWs were immersed in a solution containing HF and  $\text{AgNO}_3$  to additionally generate pores within the SiNW structure, on the basis of Au-catalyzed etching of Si. Then, the SiNWs were coated with a thin layer of carbon to enhance the electrical conductivity.

Fig. 2(d) is a porous SiNW structure prepared by a simple electrospinning process.<sup>40</sup> Electrospinning of the polymer solution, containing 1.5 g of tetraethyl orthosilicate (TEOS), 3.5 g of ethanol and 1 g of polyvinylpyrrolidone (PVP), yields  $\text{SiO}_2$  nanowires. These nanowires were then reduced by magnesium to form SiNWs. Carbon coating was then applied to increase the electrical conductivity. The SiNWs thus prepared had an average diameter of  $\sim 50 \text{ nm}$  and were highly porous.

One study<sup>41</sup> has demonstrated that SiNWs can also be synthesized by a template growth method, resulting in the nanowire structure shown in Fig. 2(e). This structure was prepared by CVD where an anodic aluminum oxide template with nano-size pores was used to guide the growth of SiNW arrays. This technique was suggested to be helpful in reducing or eliminating the Si islands that often lead to capacity fading due to stress-induced cracking and delamination.

Fig. 2(f) shows the microstructure of SiNWs that were prepared by molten-salt electrolysis.<sup>42</sup> In this process, nano- $\text{SiO}_2$  spheres was added to the molten chloride salt mixture of NaCl and  $\text{CaCl}_2$  to form the  $\text{SiO}_2$ -saturated electrolyte. During the

Table 1 Summary of SiNW electrode morphologies, parameters, capacities and performance

SiNWs electrodes No.	SiNWs architecture	Synthesis method	Electrode parameters		Summary of Electrochemical Performances					Study
			SiNWs diameter (nm)	Mass loading ( $\text{mg cm}^{-2}$ )	Max. No. of cycles run	Specific capacity at last cycle ( $\text{mA h g}^{-1}$ )	Cycles at specific capacity > 1000 ( $\text{mA h g}^{-1}$ )	Areal capacity at last cycle ( $\text{mA h cm}^{-2}$ )	Cycling potential range (V-V)	
1	Pure SiNWs	Hot-filament CVD	200	0.25	280	420	146	0.11	0.02–2	Ref. 31
2	Cu-coated SiNWs	CVD	100	0.6	50	1750	50	1.05	0.02–2	Ref. 32
3	B-doped porous SiNWs	Chemical etching	120	0.3	2000	1000	2000	0.30	0.01–2	Ref. 33
4	50% kinked SiNWs	Chemical etching	120	1.3	60	1010	60	1.31	0.01–2	Ref. 34
5	Crystalline-amorphous core shell SiNWs	CVD	125	0.2	100	1060	100	0.21	0.15–2	Ref. 35
6	Carbon nanotube enhanced SiNWs	CVD	45	0.32	35	3125	35	1.00	0.02–1.5	Ref. 36
7	SiNWs fabric	SFLS	10–50	1.17	100	500	0	0.585	0.01–3	Ref. 37
8	Carbon-coated SiNWs mixed with MWNTs	SFLS	25	0.2	75	1000	75	0.2	0.01–1	Ref. 38
9	Coral-like SiNWs	PECVD and acid etching	300	0.85	500	1250	500	1.0625	0.005–1.5	Ref. 39
10	Porous SiNWs	Electrospinning	300	1	50	1400	50	1.4	0.001–1.5	Ref. 40
11	Template-grown SiNWs	CVD with $\text{Al}_2\text{O}_3$ template	100	0.04	1100	1000	1000	0.04	0.02–1.5	Ref. 41
12	Electrodeposited SiNWs	Molten salt electrolysis	20–30	1	200	1265	200	1.265	0.01–1.5	Ref. 42

electrolysis of this mixture using the graphite anode and Ag/AgCl reference electrode, the SiNWs were directly deposited on a carbon cloth. SiNWs prepared by this method had an average diameter of  $\sim 20$  nm with an ultrathin oxide layer ( $<1$  nm as measured from TEM) on the surface. The small diameter of SiNWs is advantageous, because it can facilitate rapid  $\text{Li}^+$  diffusion in Si. The oxidation layer, because of its very small thickness relative to the SiNW diameter, is not likely to affect the electrochemical cycling performance of this SiNW electrode.

### 3. Analysis of relative merits of SiNW electrodes in Li-ion cells

The structural parameters and electrochemical performances of selected Si nanowire-based electrodes, including specific capacity, areal capacity and Si mass loading, are compiled in Table 1. Electrode capacities are expressed by two different measures: specific capacity ( $\text{mA h g}^{-1}$ ) and areal capacity ( $\text{mA h cm}^{-2}$ ). Specific capacity refers to the capacity per unit mass while areal capacity represents area-normalized capacity.

For all electrodes listed in Table 1, the specific capacity as a function of cycle number is plotted in Fig. 3. The plot of areal capacity *versus* cycle number is shown in Fig. 4. It can be seen that the relative merit of these electrodes changes depending on the capacity measure used for comparison.

The specific capacity and areal capacity reflect different Li storage aspects of an electrode. The differences between these two measures arise from the extent to which the electrolyte has access to Si, located farthest from the electrode–electrolyte interface, for lithiation. Specific capacity is determined by the maximum charge that can be stored/extracted per gram as the Si electrodes are lithiated/delithiated in cell cycling. The maximum specific capacity of Si ( $\sim 3850 \text{ mA h g}^{-1}$ ) is readily achieved in thin film Si electrodes because the length scale for diffusion is on the order of the film thickness ( $\sim 1 \mu\text{m}$ ) where

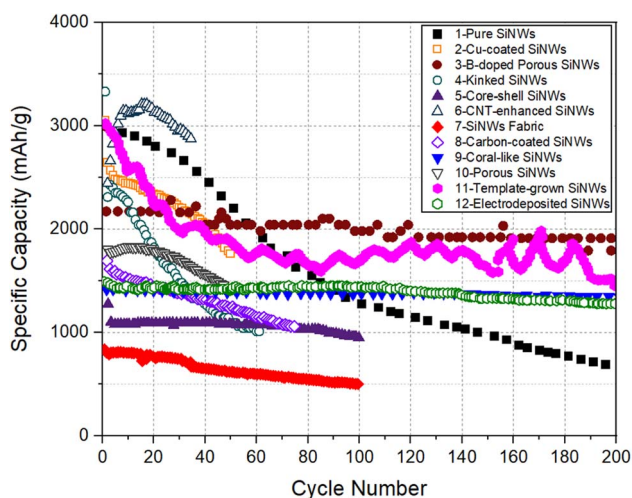


Fig. 3 Specific capacity *versus* cycle number for SiNW electrodes selected from Table 1.

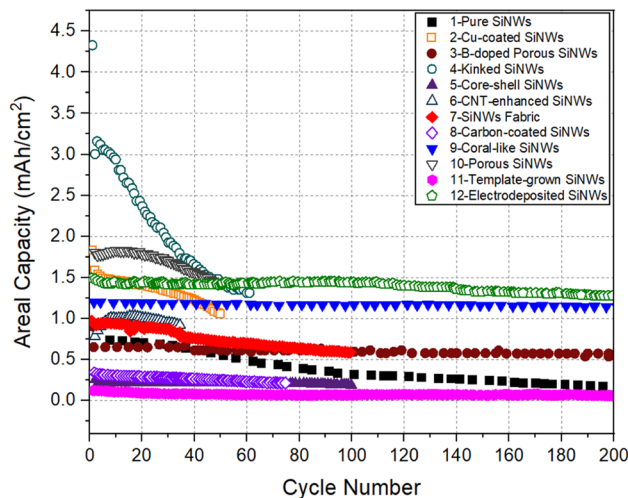


Fig. 4 Areal capacity *versus* cycle number for SiNW electrodes compared in Fig. 3.

full lithiation/delithiation of the film can be achieved even at high C rates. However, Si thin films are not viable as electrodes, because the total charge that can be stored in thin film Si is quite low and is not adequate for LIB application. The areal capacity is a better measure of electrode capacity since this captures the total charge that can be stored in the electrode. The areal capacity is simply the specific capacity multiplied by mass loading ( $\text{mg cm}^{-2}$ ).

There are two “dimensional” requirements to achieve high areal capacity in SiNW electrodes. First, a short diffusion path, as in SiNWs, would facilitate the rapid Li insertion/extraction. The second is the availability of free space between SiNWs can facilitate effective accommodation of volume change due to lithiation. More importantly, when the mass loading of Si is increased to achieve a high areal capacity, which invariably requires thicker electrodes, it is important that all Si regions have electrical contact to the base for stable cell cycling.

The data compiled in Fig. 3 are assessed based on the factors controlling the relative performances of SiNWs. First, the carbon nanotube enhanced SiNW electrode (Electrode 6) shows the highest specific capacity for up to  $\sim 50$  cycles. This extraordinary high capacity of CNT-SiNWs can be attributed to the carbon nanotubes, which ensured electrical contact between the SiNWs and the substrate and facilitating a high Li storage level.

The electrode with pure SiNWs (Electrode 1, without doping or surface modification), showed excellent specific capacity of  $>2000 \text{ mA h g}^{-1}$  for the first 50 cycles, but the capacity degraded gradually to  $\sim 700 \text{ mA h g}^{-1}$  after 200 cycles. In this work, the authors tried to improve the cycling stability by fixing the delithiation cutoff voltage to 0.8 V, instead of cycling between the conventional potential range (0.02 V–2 V). However, this only resulted in a minor improvement in specific capacity to  $\sim 900 \text{ mA h g}^{-1}$  (Table 1).

In Fig. 3, there are only a few SiNW electrodes that possessed decent specific capacity at long cycles,  $>100$ . For example, the B-

doped porous SiNW electrode (Electrode 3) possesses a relatively higher specific capacity and better cycling performance, compared to the other SiNW architectures. It is interesting to note that the specific capacity remained stable at 2000 mA h g<sup>-1</sup> after 250 cycles. This suggests that porous SiNWs structure can maintain its structural integrity after a high degree of lithiation. Electrode 11, with SiNWs grown by the template-assisted CVD method, also exhibited a comparable high specific capacity level for 200 cycles. It appears that the modified SiNW synthesis approach had helped to eliminate the Si islands that are common in the conventional CVD process. Thus, specific capacity of 1000 mA h g<sup>-1</sup> found even at the end of very long cycling period (1100 cycles, Table 1) can be explained. However, the significant fluctuations in specific capacities, resulting in several peaks and troughs indicate that the charge/discharge behavior of this SiNW electrode is not very stable.

The kinked SiNWs electrodes (Electrode 4) suffered the most severe capacity fading – the specific capacity of this electrode degraded to 1000 mA h g<sup>-1</sup> merely after 60 cycles. This indicates that the presence of kinks in SiNWs is not relevant to capacity, but potentially has a negative effect on the long-term performance. The study, however, suggested that Ni coating can improve the cycling stability of kinked SiNW electrodes by mechanical reinforcement, which remains to be seen.

We can now assess the relative performance of all the electrodes presented in Fig. 3, in terms of areal capacity. Fig. 4 presents the cycling performance of SiNW electrodes plotted in terms of areal capacity. Electrodes with kinked SiNWs (Electrode 4) started with an excellent areal capacity level (~3 mA h cm<sup>-2</sup>) in the initial cycles. This is due to the large mass loading in this electrode (1.3 mg cm<sup>-2</sup>). However, the performance was short lived with the areal capacity decreasing to ~1.3 mA h cm<sup>-2</sup> after 60 cycles. Porous SiNW electrode prepared by electrospinning on carbon cloth<sup>40</sup> (Electrode 10) also maintained a decent areal capacity of ~1.5 mA h cm<sup>-2</sup>, on average, up to 50 cycles. However, the initial impressive performances in both of these electrodes does not matter, because recently other forms of Si electrodes with areal capacities of ~3 mA h cm<sup>-2</sup> or more, cycling for a larger number of cycles, were reported.<sup>43–45</sup>

For electrode 3, although the areal capacity of the porous SiNW structure is relatively low, it shows no serious degradation in long term cycling, maintaining a modest areal capacity of ~0.5 mA h g<sup>-1</sup> after 200 cycles. Although the capacity is not impressive, the fact that it could cycle without degradation makes this structure worthy of further investigation.

From the perspective of performance after a large number of Li-ion cell cycles, SiNW electrode prepared by molten salt electrolysis (Electrode 12) emerges as the best, maintaining the highest areal capacity of 1.3 mA h g<sup>-1</sup> for about 200 cycles. It appears that the strong and conductive support structure provided by the carbon cloth in this electrode had enabled the superior performance of the electrode.

SiNWs with a Cu coating (Electrode 2) seem to have a well-balanced capacity level in terms of both specific and areal capacity metrics for 50 cycles. It was suggested<sup>32</sup> that the

presence of Cu–Si alloy layer suppresses the pulverization of SiNWs due to the volume changes of lithiation/delithiation. The Cu coating probably helps to ensure that all parts of the SiNW structure is electrically connected, thus facilitating good performance in long-term cycling. After a large number of cycles, the SiNW electrode prepared by PECVD and etching (Electrode 9) also shows a good capacity and cycling stability.<sup>39</sup> This SiNW electrode had a coral-like nanowire structure, supported by carbon coating. It shows an aerial capacity of 1.2 mA h cm<sup>-2</sup> and a specific capacity of 1200 mA h g<sup>-1</sup> for 500 cycles. Interestingly, this structure also allowed an ultra-fast charging rate of 7C, which may be attributed to the combination of interconnectedness of the nanowires, porous structure, and a highly conformal carbon coating. In this work, a full cell was fabricated with SiNW anode and commercial LiCoO<sub>2</sub> cathode, and it delivered an impressively high volumetric energy density of 1621 W h L<sup>-1</sup>.

Electrodes 7 and 8 represent SiNW electrodes prepared by solution-based SFLS synthesis. The paper-like SiNW fabric in Electrode 7 is mechanically flexible.<sup>37</sup> Despite this, the electrode showed the worst specific capacity, (<1000 mA h g<sup>-1</sup>) even in the second cycle. As this SiNW fabric electrode has a void volume of 90%, the areal capacity of ~0.6 mA h cm<sup>-2</sup> delivered by this electrode is not impressive by any standard. It was suggested that the low specific capacity and areal capacity of the SiNW fabric electrode are due to the loss of structural integrity of the SiNWs during cycling.<sup>37</sup> In Electrode 8, carbon coating and multiwalled carbon nanotubes (MWNTs) were introduced into the SiNWs during the preparation by traditional slurry casting process.<sup>38</sup> Although moderate specific capacity of ~1000 mA h g<sup>-1</sup> was seen, the presence of carbon MWNTs additives or CMC binder reduced the Si mass loading, leading to a degradation in the areal capacity. This is the reason for the very low areal capacity (~0.25 mA h cm<sup>-2</sup>) in this electrode. Therefore, solution-based route for SiNW synthesis may not be the best approach for the preparation of SiNW electrodes for LIBs.

It is also worth noting that relatively low capacity levels, by both capacity measures, were observed for the crystalline-amorphous core-shell SiNW electrodes (Electrode 5), shown in Fig. 3 and 4. This may be because of the relatively high cutoff voltage (150 mV) used in the electrochemical cycling experiments. Normally, this level is about 10–50 mV, to prevent over-lithiation of Si. The low cutoff voltage usually results in the formation of Li<sub>15</sub>Si<sub>4</sub> crystalline phase, which is thought to be responsible for a severe capacity fading in the electrodes, due to the irreversibility of phase transition from Li to Li<sub>15</sub>Si<sub>4</sub>. With a large voltage cutoff (150 mV), the formation of Li<sub>15</sub>Si<sub>4</sub> can be suppressed, which can significantly improve the cycling stability and minimize the capacity loss of the electrode. As the data<sup>35</sup> suggested, a reasonable specific capacity of 1060 mA h g<sup>-1</sup> can still be reached with a cutoff voltage of 150 mV, which is nearly three times of that with graphite electrode. However, the c-a core-shell SiNW electrodes showed<sup>35</sup> a capacity as high as 2500 mA h g<sup>-1</sup> within 30 cycles, when a low cutoff voltage (10 mV) was used during cycling.

## 4. The effects of mass loading of SiNWs on capacity

To assess the effect of Si mass loading on the Li-storage capacities, the areal capacity and specific capacity at 50 cycles, for the electrodes considered here, were plotted as a function of SiNW mass loading in Fig. 5 and 6, respectively. The data in both plots approximately show a linear correlation with a few exceptions. In Fig. 5, there is a clear trend showing that the increase of mass loading can lead to the increase in the areal capacity of SiNW electrodes. On the other hand, Fig. 6 shows that the increase in Si mass loading is not desirable for the achievement of high specific capacity in SiNWs. The two different behaviors can be explained based on kinetics. The increase of active Si mass on the electrode per unit area leads to

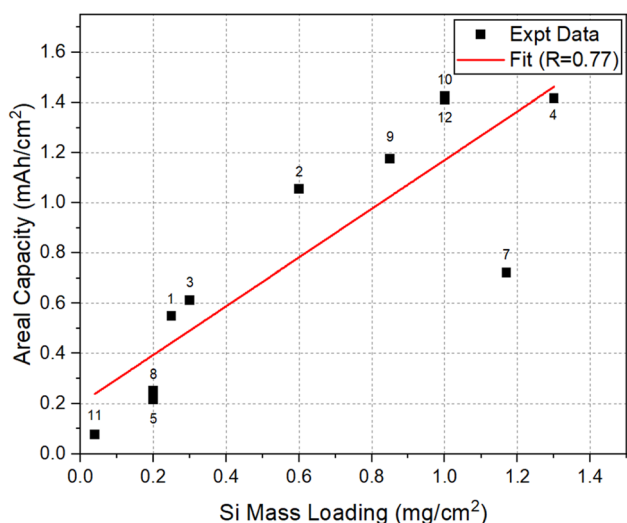


Fig. 5 Areal capacity versus Si mass loading at 50 cycles for the selected electrodes listed in Table 1.

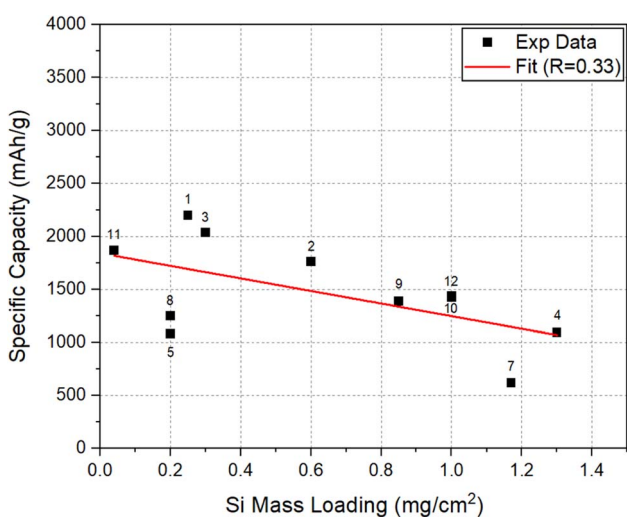


Fig. 6 Specific capacity versus Si mass loading at 50 cycles for the electrodes compared in Fig. 5.

the thickening of Si features in the electrode. However, a relatively thicker Si means an increase in the distance for Li-ion transport<sup>46,47</sup> during lithiation/delithiation. Thus, the kinetic limitations of Li–Si reaction will come into play. In the worst-case scenario, a significant portion of the Si in thick electrode may not be involved in the lithiation/delithiation. This will be most significant especially at high C-rates. In addition, a thick electrode requires a high structural support to it to be stable in cycling, since the accumulation of volume expansion in thicker Si electrodes, upon lithiation, may lead to cracking and fragmentation<sup>48–51</sup> of the electrode. This is also supported by the fact that most of the works that reported high specific capacity and excellent cycling performance in Si were for relatively thin electrodes with a mass loading less than 1 mg cm<sup>-2</sup>.<sup>52</sup>

It is to be noted that the SiNW electrodes compiled in this review are from different studies. It is possible that small differences in electrode architectures (beyond that is seen in the micrographs, Fig. 1 and 2), electrode fabrication process (purity and contamination of SiNWs) and cycling conditions (potential limits) can aggravate the differences between the electrochemical performances. These factors are likely to be responsible for the relative differences between some SiNW electrodes in the capacity vs. mass loading plots shown in Fig. 5 and 6.

## 5. SiNW electrodes vs. Si electrodes with other forms of silicon

It will be informative to compare the performance of SiNW electrodes with other forms of Si to highlight the potential of SiNW electrodes in the quest for high capacity negative electrodes for Li-ion batteries. For this purpose, Electrode 1 (pure SiNWs) which has the relatively high specific capacity and Electrode 4 (kinked SiNWs), which has a relatively high areal capacity are chosen for comparison with the cycling data of Si nanoparticle electrode,<sup>53</sup> Si thin film electrode<sup>54</sup> and columnar Si electrode.<sup>55</sup>

Fig. 7 and 8 shows the specific capacity and the areal capacity of different forms of Si electrodes for 50 cycles, respectively. It can be seen that the Si thin film electrode shows a superior specific capacity of  $\sim 3000$  mA h g<sup>-1</sup> with a high cycling stability, which is readily explainable, due to small film thickness ( $\sim 450$  nm). It is noteworthy that the specific capacity of SiNW electrode is lower than that of the Si thin film, but higher than that of the Si nanoparticle electrode and columnar Si electrode. In contrast, as shown in Fig. 8, the Si thin film electrode has a much lower areal capacity than the other Si electrodes. Evidently, this is because of the low mass loading of the thin film electrode due to its limited thickness ( $\sim 450$  nm). Thin films with low mass loading are not relevant for the practical application in LIBs but are useful for basic research. The Si nanoparticle electrode shows the highest areal capacity of 2 mA h cm<sup>-2</sup>, followed by the SiNW electrode ( $\sim 1.4$  mA h cm<sup>-2</sup>) and then the columnar Si electrode ( $\sim 1.3$  mA h cm<sup>-2</sup>). Therefore, it is clear that SiNW electrodes can deliver a comparable or higher capacity levels, in terms of both capacity measures, relative to well-performing Si nanoparticle electrodes. The



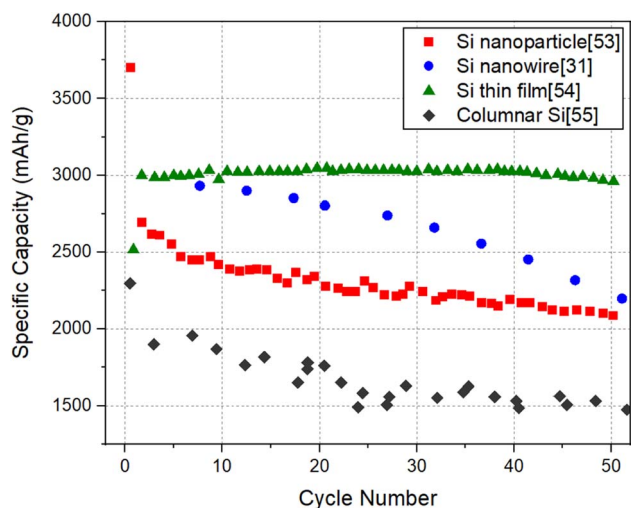


Fig. 7 Comparison of different morphologies of Si electrodes in terms of specific capacity.

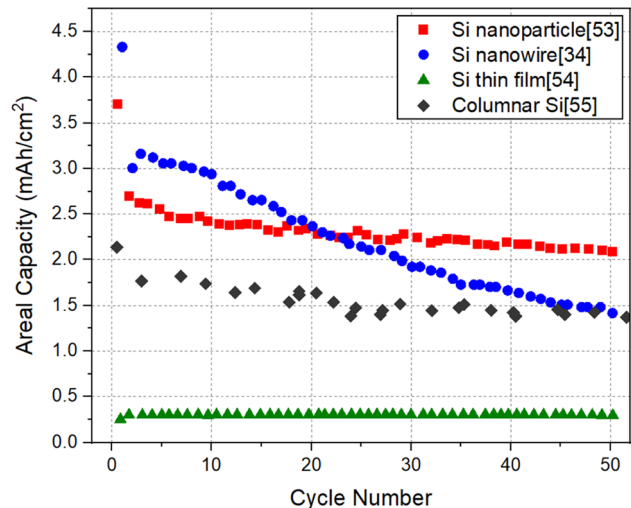


Fig. 8 Comparison of different morphologies of Si electrodes in terms of areal capacity.

comparison brings out the fact that for LIB applications requiring minimal weight, SiNW electrodes may be the best option. For the applications where the size of the battery system matters the most, Si nanoparticle electrodes are more favorable, but only slightly better than SiNWs.

## 6. Future prospects for SiNW electrodes

The SiNW electrodes have a great potential for Li-ion batteries, principally due to their ability to rapidly get lithiated/delithiated (less kinetic barrier), and their ability to accommodate volume expansion in the lateral porous space between the nanowires. The large variety of SiNW synthesis routes provides a significant hope for the development of commercially-viable SiNW

electrodes with high Li-storage capacity and good cycling stability. In particular, for SiNWs grown by CVD and solution-based techniques, electrode fabrication can be achieved *via* the traditional slurry casting process, which is compatible with the current production process of LIB electrodes. Also, as in the case of SiNWs prepared by etching the Si wafer substrate, the electrode can be cut directly from the etched wafer without the need of conductive additives and binders, which can enable easy integration in electronic components, for example, in on-chip batteries.

Further optimization of the SiNW electrodes needs to focus on simplification of the SiNW growth techniques, the enhancement of their cycling stability and lowering the cost for manufacturing. With the improved understanding of lithiation/delithiation behaviors of SiNWs, it is probable that the high capacity SiNW electrodes will play a significant role in the development of next-generation LIBs.

## 7. Conclusions

1. Si nanowire-based electrodes prepared by different synthesis approaches were compared and evaluated in terms of specific capacity, areal capacity and cycling performance. It is seen that process modifications, including surface coating, doping or steps that enable the growth of porous and core-shell structures, have measurable impact on the electrochemical performances of SiNW electrodes. Thus, further improvements in SiNW electrodes can lead to high Li-storage capacity levels needed in future LIBs.

2. To assess the true merit of a SiNW structure, one needs to compare the electrodes both in terms of specific capacity and areal capacity measures. Publications that report the outstanding specific capacities of Si electrodes should be carefully evaluated and the areal capacities of reported structures should be verified to see if a structure truly provides meaningful Li storage levels.

3. In SiNW electrodes, the areal capacity and specific capacity of SiNW electrodes are closely related to the Si mass loading. A large mass loading is found to lead to a high areal capacity, but the small mass loading is found to lead to a high specific capacity.

4. SiNW electrodes, when evaluated against other forms of Si electrodes, shows relatively high and well-balanced specific capacity and areal capacity levels that are of interest for practical Li-ion batteries. Therefore, with further development, SiNW electrodes have a bright future as a negative electrode with high Li storage capacity in Li-ion batteries, provided a reduction in manufacturing cost is achieved.

## Data availability statement

The raw data used in this review article are available in the references listed in Table 1. The processed data used in making the plots here are available from the first author upon request.

## Conflicts of interest

The authors declare that they have no known competing financial interests or personal relationships that could have appeared to influence the work reported in this paper.

## Acknowledgements

The research was supported by DE Office of Science, Program on Neutron Scattering, through the grant: DE-SC0019056.

## References

- 1 A. Manthiram, An Outlook on Lithium Ion Battery Technology, *ACS Cent. Sci.*, 2017, **3**(10), 1063–1069, DOI: [10.1021/acscentsci.7b00288](https://doi.org/10.1021/acscentsci.7b00288).
- 2 L. Leveau, *et al.*, Silicon Nano-Trees as High Areal Capacity Anodes for Lithium-Ion Batteries, *J. Power Sources*, 2016, **316**, 1–7, DOI: [10.1016/j.jpowsour.2016.03.053](https://doi.org/10.1016/j.jpowsour.2016.03.053).
- 3 U. Kasavajjula, *et al.*, Nano- and Bulk-Silicon-Based Insertion Anodes for Lithium-Ion Secondary Cells, *J. Power Sources*, 2007, **163**(2), 1003–1039, DOI: [10.1016/j.jpowsour.2006.09.084](https://doi.org/10.1016/j.jpowsour.2006.09.084).
- 4 T. L. Kulova, *et al.*, Lithium Insertion into Amorphous Silicon Thin-Film Electrodes, *J. Electroanal. Chem.*, 2007, **600**(1), 217–225, DOI: [10.1016/j.jelechem.2006.07.002](https://doi.org/10.1016/j.jelechem.2006.07.002).
- 5 T. Yoon, *et al.*, Capacity Fading Mechanisms of Silicon Nanoparticle Negative Electrodes for Lithium Ion Batteries, *J. Electrochem. Soc.*, 2015, **162**(12), A2325, DOI: [10.1149/2.0731512jes](https://doi.org/10.1149/2.0731512jes).
- 6 H. Wu, *et al.*, Engineering Empty Space between Si Nanoparticles for Lithium-Ion Battery Anodes, *Nano Lett.*, 2012, **12**(2), 904–909, DOI: [10.1021/nl203967r](https://doi.org/10.1021/nl203967r).
- 7 Y. Yang, *et al.*, Silicon-Nanoparticle-Based Composites for Advanced Lithium-Ion Battery Anodes, *Nanoscale*, 2020, **12**(14), 7461–7484, DOI: [10.1039/c9nr10652a](https://doi.org/10.1039/c9nr10652a).
- 8 C. K. Chan, *et al.*, High-Performance Lithium Battery Anodes Using Silicon Nanowires, *Nat. Nanotechnol.*, 2007, **3**(1), 31–35, DOI: [10.1038/nnano.2007.411](https://doi.org/10.1038/nnano.2007.411).
- 9 V. Etacheri, *et al.*, Effect of Fluoroethylene Carbonate (FEC) on the Performance and Surface Chemistry of Si-Nanowire Li-Ion Battery Anodes, *Langmuir*, 2011, **28**(1), 965–976, DOI: [10.1021/la203712s](https://doi.org/10.1021/la203712s).
- 10 M. T. McDowell, *et al.*, Novel Size and Surface Oxide Effects in Silicon Nanowires as Lithium Battery Anodes, *Nano Lett.*, 2011, **11**(9), 4018–4025, DOI: [10.1021/nl202630n](https://doi.org/10.1021/nl202630n).
- 11 N.-S. Choi, *et al.*, Effect of Fluoroethylene Carbonate Additive on Interfacial Properties of Silicon Thin-Film Electrode, *J. Power Sources*, 2006, **161**(2), 1254–1259, DOI: [10.1016/j.jpowsour.2006.05.049](https://doi.org/10.1016/j.jpowsour.2006.05.049).
- 12 T. L. Kulova, *et al.*, Lithium Insertion into Amorphous Silicon Thin-Film Electrodes, *J. Electroanal. Chem.*, 2007, **600**(1), 217–225, DOI: [10.1016/j.jelechem.2006.07.002](https://doi.org/10.1016/j.jelechem.2006.07.002).
- 13 E. Markevich, *et al.*, Amorphous Columnar Silicon Anodes for Advanced High Voltage Lithium Ion Full Cells: Dominant Factors Governing Cycling Performance, *J. Electrochem. Soc.*, 2013, **160**(10), A1824, DOI: [10.1149/2.085310jes](https://doi.org/10.1149/2.085310jes).
- 14 B. Vadlamani, *et al.*, Large Effect of Structural Variations in the Columnar Silicon Electrode on Energy Storage Capacity and Electrode Structural Integrity in Li-Ion Cells, *J. Mater. Res.*, 2020, **35**(21), 2976–2988, DOI: [10.1557/jmr.2020.266](https://doi.org/10.1557/jmr.2020.266).
- 15 M. Ashuri, *et al.*, Silicon as a Potential Anode Material for Li-Ion Batteries: Where Size, Geometry and Structure Matter, *Nanoscale*, 2016, **8**(1), 74–103, DOI: [10.1039/c5nr05116a](https://doi.org/10.1039/c5nr05116a).
- 16 L. Hu, *et al.*, Si Nanoparticle-Decorated Si Nanowire Networks for Li-Ion Battery Anodes, *Chem. Commun.*, 2011, **47**(1), 367–369, DOI: [10.1039/c0cc02078h](https://doi.org/10.1039/c0cc02078h).
- 17 X.-L. Wang and W.-Q. Han, Graphene Enhances Li Storage Capacity of Porous Single-Crystalline Silicon Nanowires, *ACS Appl. Mater. Interfaces*, 2010, **2**(12), 3709–3713, DOI: [10.1021/am100857h](https://doi.org/10.1021/am100857h).
- 18 S. Misra, *et al.*, In Situ X-Ray Diffraction Studies of (De) Lithiation Mechanism in Silicon Nanowire Anodes, *ACS Nano*, 2012, **6**(6), 5465–5473, DOI: [10.1021/nn301339g](https://doi.org/10.1021/nn301339g).
- 19 X.-L. Wang and W.-Q. Han, Graphene Enhances Li Storage Capacity of Porous Single-Crystalline Silicon Nanowires, *ACS Appl. Mater. Interfaces*, 2010, **2**(12), 3709–3713, DOI: [10.1021/am100857h](https://doi.org/10.1021/am100857h).
- 20 X. Su, *et al.*, Silicon-Based Nanomaterials for Lithium-Ion Batteries: A Review, *Adv. Energy Mater.*, 2013, **4**(1), 1300882, DOI: [10.1002/aenm.201300882](https://doi.org/10.1002/aenm.201300882).
- 21 Z. Huang, *et al.*, Metal-Assisted Chemical Etching of Silicon: A Review, *Adv. Mater.*, 2010, **23**(2), 285–308, DOI: [10.1002/adma.201001784](https://doi.org/10.1002/adma.201001784).
- 22 H.-D. Um, *et al.*, Versatile Control of Metal-Assisted Chemical Etching for Vertical Silicon Microwire Arrays and Their Photovoltaic Applications, *Sci. Rep.*, 2015, **5**(1), 11277, DOI: [10.1038/srep11277](https://doi.org/10.1038/srep11277).
- 23 X. Wang, *et al.*, Carbon-Coated Silicon Nanowires on Carbon Fabric as Self-Supported Electrodes for Flexible Lithium-Ion Batteries, *ACS Appl. Mater. Interfaces*, 2017, **9**(11), 9551–9558, DOI: [10.1021/acsami.6b12080](https://doi.org/10.1021/acsami.6b12080).
- 24 M. C. Qiu, *et al.*, Fabrication of Ordered NiO Coated Si Nanowire Array Films as Electrodes for a High Performance Lithium Ion Battery, *ACS Appl. Mater. Interfaces*, 2010, **2**(12), 3614–3618, DOI: [10.1021/am100791z](https://doi.org/10.1021/am100791z).
- 25 W. McSweeney, *et al.*, Metal-Assisted Chemical Etching of Silicon and the Behavior of Nanoscale Silicon Materials as Li-Ion Battery Anodes, *Nano Res.*, 2015, **8**(5), 1395–1442, DOI: [10.1007/s12274-014-0659-9](https://doi.org/10.1007/s12274-014-0659-9).
- 26 H. Wu and Y. Cui, Designing Nanostructured Si Anodes for High Energy Lithium Ion Batteries, *Nano Today*, 2012, **7**(5), 414–429, DOI: [10.1016/j.nantod.2012.08.004](https://doi.org/10.1016/j.nantod.2012.08.004).
- 27 A. D. Refino, *et al.*, Versatilely Tuned Vertical Silicon Nanowire Arrays by Cryogenic Reactive Ion Etching as a Lithium-Ion Battery Anode, *Sci. Rep.*, 2021, **11**(1), 19779, DOI: [10.1038/s41598-021-99173-4](https://doi.org/10.1038/s41598-021-99173-4).
- 28 A. P. Nugroho, *et al.*, Vertically Aligned N-Type Silicon Nanowire Array as a Free-Standing Anode for Lithium-Ion Batteries, *Nanomaterials*, 2021, **11**(11), 3137, DOI: [10.3390/nano11113137](https://doi.org/10.3390/nano11113137).

- 29 M. R. Zamfir, *et al.*, Silicon Nanowires for Li-Based Battery Anodes: A Review, *J. Mater. Chem. A*, 2013, **1**(34), 9566, DOI: [10.1039/c3ta11714f](https://doi.org/10.1039/c3ta11714f).
- 30 Y. Yang, *et al.*, A Review on Silicon Nanowire-Based Anodes for next-Generation High-Performance Lithium-Ion Batteries from a Material-Based Perspective, *Sustainable Energy Fuels*, 2020, **4**(4), 1577–1594, DOI: [10.1039/c9se01165j](https://doi.org/10.1039/c9se01165j).
- 31 L. Leveau, *et al.*, Cycling Strategies for Optimizing Silicon Nanowires Performance as Negative Electrode for Lithium Battery, *Electrochim. Acta*, 2015, **157**, 218–224, DOI: [10.1016/j.electacta.2015.01.037](https://doi.org/10.1016/j.electacta.2015.01.037).
- 32 H. Chen, *et al.*, Silicon Nanowires Coated with Copper Layer as Anode Materials for Lithium-Ion Batteries, *J. Power Sources*, 2011, **196**(16), 6657–6662, DOI: [10.1016/j.jpowsour.2010.12.075](https://doi.org/10.1016/j.jpowsour.2010.12.075).
- 33 M. Ge, *et al.*, Porous Doped Silicon Nanowires for Lithium Ion Battery Anode with Long Cycle Life, *Nano Lett.*, 2012, **12**(5), 2318–2323, DOI: [10.1021/nl300206e](https://doi.org/10.1021/nl300206e).
- 34 G. Sandu, *et al.*, Kinked Silicon Nanowires-Enabled Interweaving Electrode Configuration for Lithium-Ion Batteries, *Sci. Rep.*, 2018, **8**(1), 9794, DOI: [10.1038/s41598-018-28108-3](https://doi.org/10.1038/s41598-018-28108-3).
- 35 Li-F. Cui, *et al.*, Crystalline-Amorphous Core-Shell Silicon Nanowires for High Capacity and High Current Battery Electrodes, *Nano Lett.*, 2009, **9**(1), 491–495, DOI: [10.1021/nl8036323](https://doi.org/10.1021/nl8036323).
- 36 X. Li, *et al.*, Carbon Nanotube-Enhanced Growth of Silicon Nanowires as an Anode for High-Performance Lithium-Ion Batteries, *Adv. Energy Mater.*, 2011, **2**(1), 87–93, DOI: [10.1002/aenm.201100519](https://doi.org/10.1002/aenm.201100519).
- 37 A. M. Chockla, *et al.*, Silicon Nanowire Fabric as a Lithium Ion Battery Electrode Material, *J. Am. Chem. Soc.*, 2011, **133**(51), 20914–20921, DOI: [10.1021/ja208232h](https://doi.org/10.1021/ja208232h).
- 38 C. K. Chan, *et al.*, Solution-Grown Silicon Nanowires for Lithium-Ion Battery Anodes, *ACS Nano*, 2010, **4**(3), 1443–1450, DOI: [10.1021/nn901409q](https://doi.org/10.1021/nn901409q).
- 39 B. Wang, *et al.*, Ultrafast-Charging Silicon-Based Coral-like Network Anodes for Lithium-Ion Batteries with High Energy and Power Densities, *ACS Nano*, 2019, **13**(2), 2307–2315, DOI: [10.1021/acsnano.8b09034.s001](https://doi.org/10.1021/acsnano.8b09034.s001).
- 40 J.-K. Yoo, *et al.*, Porous Silicon Nanowires for Lithium Rechargeable Batteries, *Nanotechnology*, 2013, **24**(42), 424008, DOI: [10.1088/0957-4484/24/42/424008](https://doi.org/10.1088/0957-4484/24/42/424008).
- 41 J.-H. Cho and S. Tom Picraux, Enhanced Lithium Ion Battery Cycling of Silicon Nanowire Anodes by Template Growth to Eliminate Silicon Underlayer Islands, *Nano Lett.*, 2013, **13**(11), 5740–5747, DOI: [10.1021/nl4036498](https://doi.org/10.1021/nl4036498).
- 42 W. Weng and W. Xiao, Electrodeposited Silicon Nanowires from Silica Dissolved in Molten Salts as a Binder-Free Anode for Lithium-Ion Batteries, *ACS Appl. Energy Mater.*, 2018, **2**(1), 804–813, DOI: [10.1021/acsaem.8b01870](https://doi.org/10.1021/acsaem.8b01870).
- 43 Z. Chen, *et al.*, High-Areal-Capacity Silicon Electrodes with Low-Cost Silicon Particles Based on Spatial Control of Self-Healing Binder, *Adv. Energy Mater.*, 2015, **5**(8), 1401826, DOI: [10.1002/aenm.201401826](https://doi.org/10.1002/aenm.201401826).
- 44 M. Marinaro, *et al.*, Toward Pre-Lithified High Areal Capacity Silicon Anodes for Lithium-Ion Batteries, *Electrochim. Acta*, 2016, **206**, 99–107, DOI: [10.1016/j.electacta.2016.03.139](https://doi.org/10.1016/j.electacta.2016.03.139).
- 45 L. Hu, *et al.*, Design of High-Energy-Dissipation, Deformable Binder for High-Areal-Capacity Silicon Anode in Lithium-Ion Batteries, *Chem. Eng. J.*, 2021, **420**, 129991, DOI: [10.1016/j.cej.2021.129991](https://doi.org/10.1016/j.cej.2021.129991).
- 46 H. Li, *et al.*, Ultra-Thick Graphene Bulk Supercapacitor Electrodes for Compact Energy Storage, *Energy Environ. Sci.*, 2016, **9**(10), 3135–3142, DOI: [10.1039/c6ee00941g](https://doi.org/10.1039/c6ee00941g).
- 47 J. S. Sander, *et al.*, High-Performance Battery Electrodes via Magnetic Templating, *Nat. Energy*, 2016, **1**(8), 16099, DOI: [10.1038/nenergy.2016.99](https://doi.org/10.1038/nenergy.2016.99).
- 48 J. Han, *et al.*, A Thick Yet Dense Silicon Anode with Enhanced Interface Stability in Lithium Storage Evidenced by In Situ Tem Observations, *Sci. Bull.*, 2020, **65**(18), 1563–1569, DOI: [10.1016/j.scib.2020.05.018](https://doi.org/10.1016/j.scib.2020.05.018).
- 49 S. Chae, *et al.*, Confronting Issues of the Practical Implementation of Si Anode in High-Energy Lithium-Ion Batteries, *Joule*, 2017, **1**(1), 47–60, DOI: [10.1016/j.joule.2017.07.006](https://doi.org/10.1016/j.joule.2017.07.006).
- 50 J. Wang, *et al.*, Shell-Protective Secondary Silicon Nanostructures as Pressure-Resistant High-Volumetric-Capacity Anodes for Lithium-Ion Batteries, *Nano Lett.*, 2018, **18**(11), 7060–7065, DOI: [10.1021/acsnanolett.8b03065](https://doi.org/10.1021/acsnanolett.8b03065).
- 51 Z. Xu, *et al.*, Silicon Microparticle Anodes with Self-Healing Multiple Network Binder, *Joule*, 2018, **2**(5), 950–961, DOI: [10.1016/j.joule.2018.02.012](https://doi.org/10.1016/j.joule.2018.02.012).
- 52 X. Zhao and V.-P. Lehto, Challenges and Prospects of Nanosized Silicon Anodes in Lithium-Ion Batteries, *Nanotechnology*, 2020, **32**(4), 042002, DOI: [10.1088/1361-6528/abb850](https://doi.org/10.1088/1361-6528/abb850).
- 53 T. M. Higgins, *et al.*, A Commercial Conducting Polymer as Both Binder and Conductive Additive for Silicon Nanoparticle-Based Lithium-Ion Battery Negative Electrodes, *ACS Nano*, 2016, **10**(3), 3702–3713, DOI: [10.1021/acsnano.6b00218](https://doi.org/10.1021/acsnano.6b00218).
- 54 H. Kim, *et al.*, Recent Advances in the Si-Based Nanocomposite Materials as High Capacity Anode Materials for Lithium Ion Batteries, *Mater. Today*, 2014, **17**(6), 285–297, DOI: [10.1016/j.mattod.2014.05.003](https://doi.org/10.1016/j.mattod.2014.05.003).
- 55 K. S. Ravi Chandran and J. Palmer, A Critical Review and Assessment of 3D Columnar Silicon Electrode Architectures and Their Performance as Negative Electrodes in Li-Ion Cells, *Mater. Sci. Eng. B*, 2021, **271**, 115278, DOI: [10.1016/j.mseb.2021.115278](https://doi.org/10.1016/j.mseb.2021.115278).